

AN EXPERIMENTAL STUDY OF THE INTERFACIAL FRICTION FACTOR FOR COUNTERCURRENT STRATIFIED AIR-WATER FLOW IN NEARLY HORIZONTAL AND INCLINED PIPES

Seon-Oh Yu, Yang-Seok Kim, and Moon-Hyun Chun

Korea Advanced Institute of Science and Technology

Chang-Kyung Sung and Sang-Doug Park

Korea Electric Power Corporation

Byung-Ryung Lee and Yong-Soo Sohn

Korea Atomic Energy Research Institute

Abstract

The Interfacial friction factor for the countercurrent stratified air-water flow has been experimentally investigated in nearly horizontal and inclined pipes. The presence of the hydraulic jump may significantly affect both the flow pattern and the interfacial friction factor. The measured values of f_i in nearly horizontal and two inclined pipes are of the same order of magnitude but the dependencies of the air and water velocities are slightly different.

I. Introduction

The interfacial friction factor, f_i , has been considered as an essential closure relationship for two-phase flow. This quantity is needed in the analysis of the following two phase flow phenomena in particular : flow transition criteria including the flooding point, the process of mass, momentum, and heat transfer in stratified flow, the condensation-induced waterhammer (CIWH) in a long horizontal pipe, and two-phase flow pressure drops. A number of correlations for cocurrent and countercurrent stratified two-phase flow have been proposed as summarized in Table 1. However, the effect of the inclination angle on f_i has rarely been studied until recently. The objective of present experimental work is : (1) to investigate experimentally the flow characteristics of countercurrent stratified air-water flow for nearly horizontal and slightly inclined pipes ($\theta = 1^\circ$ and 2° from the horizontal), and (2) to measure and compare the interfacial friction factors for three different types of the test sections.

II. Experimental Works

A schematic diagram of the present test facility to simulate the countercurrent stratified air-water flow is shown in Fig. 1. The test facility consists of a test section, an air/water supply system, instrumentations, and data acquisition system. The test section is a tube (2m in full length and 0.05m in inner diameter) and both ends have a simple sharp-edge. An acrylic tube is used for flow visualizaion. To form a countercurrent flow, the filtered water is pumped from the water surge tank to the test section while the air is supplied through the air reservoir to the test section by the belt-type blower. The uniform flow of water is achieved by installing the honeycomb and various size mesh screens in the water reservoir. The flow rates of air and water are monitored by four and three rotameters, respectively.

The water level is measured using two-parallel wire conductance probes which are located at $L/D = 1.2, 21.5,$ and 22.1 , where L/D denotes the dimensionless distance from the water inlet (in this paper, the water level measured at $L/D = 22.1$ will be presented). Prior to the experiment, static calibration has been performed for the output signal of each conductance probe, in which the signals for various water levels are compared with the reference water level measured by a slide caliper with an accuracy of 0.02mm . The typical calibration curves of probes are shown in Fig. 2. Pressure drop in the gas phase between the positions of $L/D = 1.0$ and 44.0 has been measured by the differential pressure transmitter with a full scale of 0.05m water column (1245.6Pa) and accuracy within $\pm 0.025\%$.

A series of experiments have been made fixing the water flow rate and increasing the air flow rate by small increments until a slug is formed within the nearly horizontal test section. For all the tests, sufficient time is allowed to measure the instantaneous pressure drop and water levels, and the events in the test section are observed. This procedure is repeated for other water flow rates and other inclination angles of test section. A desired inclination angle is obtained by lowering the air reservoir. In this work, the ranges of the superficial water velocity, j_f , and the superficial air velocity, j_g , are $0.01273\sim 0.13581\text{m/s}$ and $0.679\sim 6.791\text{m/s}$, respectively. All the tests are conducted at atmospheric condition, and during each test, the air and water temperatures are kept in the range of $23\sim 24^\circ\text{C}$ and $20\sim 22^\circ\text{C}$, respectively.

III. Results and Discussion

3.1 Visual Observations

The variation of the flow pattern with the increase in the air flow rate shows a distinct difference between nearly horizontal and inclined pipe tests. For nearly horizontal tests, the observed flow patterns are stratified-smooth, 2-D, 3-D, roll waves, and slugging. For two inclined pipe tests, however, the roll waves are not observed. Figure 3 shows typical time-responses of the instantaneous pressure drop and water level for $j_f = 0.0679\text{m/s}$.

3.1.1 Nearly Horizontal Tests

For a fixed water flow rate with no air flow, there exist two distinct water levels which can be identified as what is called hydraulic jump. The upstream level with respect to the water flow is lower than the downstream level and this hydraulic jump slowly moves toward the inlet of the water flow as the air flow rate is increased.

For the low water flow rate ($< 5.0 \times 10^{-5}\text{m}^3/\text{s}$), the flow is smooth until the waves appear on the interface. These waves propagate to the water inlet by air shear stress in the downstream region, causing the pressure drop and water level to increase. For sufficiently high air flow rate, the hydraulic jump disappears in the pipe, and waves become regular and have the shape of the roll wave. At the air flow rate close to the transition to the slug flow, the flow becomes very unstable and, then, subsequently slug is observed. For the high water flow rate ($\geq 5.0 \times 10^{-5}\text{m}^3/\text{s}$), however, roll waves are observed only in the downstream region because the hydraulic jump still exists within the pipe even when the air flow rate is close to the critical flow rate for the slug occurrence. It is worth noting that the major portion of the air momentum is concentrated on the steepest region instead of the water wave on the interface in the upstream region. Thus, the slight increase of the air flow rate close to the onset of slugging results in breaking the edge of the steepest region. As time passes, the water level in the water reservoir is much higher than the level in the pipe and the water flow is abruptly choked at the water inlet.

3.1.2 Slightly Inclined Tests

Slightly inclined tests show some different flow characteristics from nearly horizontal tests because the gravitational force cannot be neglected. In these tests, the prevailing flow pattern is a 3-D wave flow. At very high air flow rate, the hydraulic jump occurs near the water outlet. It should be noted that the slug occurs as soon as the hydraulic jump is initiated near the water outlet. The observed hydraulic jump has a similar feature as in the nearly horizontal tests but the difference of two water levels is not so large. Waves of long-wavelength and high-amplitude in the downstream region are observed to be very unstable and irregular, while waves in the upstream region are still three dimensional. Near the onset of slugging, it is very difficult to identify the hydraulic jump because the water maintains almost the same level in the entire pipe and the waves move back and forth. For example, waves traveling to the water outlet move to the water inlet due to the air flow and, then, to the water outlet due to the gravitational force. The slug seems to occur through the following processes: a standstill of one of the 3-D waves, growth, and formation of a fast-moving slug. For the high water flow rate, the choking of the water flow is observed as in nearly horizontal tests.

3.2 Time-Averaged Water Level

For nearly horizontal pipes, an abrupt increase in the water level is observed with increasing j_g . This can be interpreted as follows: As j_g is increased, the hydraulic jump moving toward the water inlet passes through the conductance probe and, therefore, the measured water level increases abruptly. In the slightly inclined pipes, however, the effect of j_g on the water level is almost negligible within the present test range. As expected, the water level decreases with an increase in the inclination angle of the test section.

3.3 Interfacial Friction Factor

Assuming that the pressure drop varies linearly with the length of pipe, the interfacial friction factor, f_i , can be evaluated from the gas-phase momentum equation for fully developed countercurrent stratified two-phase flow as follows:

$$f_i = \frac{1}{S_i V_r^2} \left(\frac{2A_g \Delta P}{\rho_g L} - f_g S_g V_g^2 - 2A_g g \sin \theta \right) \quad (1)$$

where S_i is the interface width, $V_r = V_g + V_f$, the relative velocity, V_g , the gas velocity, V_f , the water velocity, A_g , the fractional area occupied by the water, ΔP , the pressure drop, ρ_g , the density of the air, L , the length of the test section, S_g , the peripheral length of the air, g , the acceleration of the gravity, and θ , the inclination angle of the test section. Since the single-phase pressure drop data obtained only for the air flow with the present test section show reasonably good agreement with the Blasius equation as shown in Fig. 4, the gas-to-wall friction factor, f_g , is determined from the Blasius equation.

Figure 5a shows that the value of $(f_i/f_g)_{\text{exp}}$ increases gradually with increase in V_r until V_r reaches a value between 3~4m/s. Beyond this point, $(f_i/f_g)_{\text{exp}}$ decreases sharply when j_f is high. These results may be due to the presence of the hydraulic jump within the nearly horizontal pipe. In this case, the water level used in the determination of $(f_i/f_g)_{\text{exp}}$ increases greatly which causes $(f_i/f_g)_{\text{exp}}$ to decrease. For inclined pipe tests as shown in Figs. 5b and 5c, however, $(f_i/f_g)_{\text{exp}}$ continues to increase with increase in V_r , but the maximum $(f_i/f_g)_{\text{exp}}$ value under the present experimental condition is less than 4.0 (or $(f_i)_{\text{exp}} = 0.025$). It should be noted that Lee [7] reported f_i in air-water and steam-water countercurrent flows is always less than 0.015 regardless of the flow condition.

In Fig. 6, the present experimental data for nearly horizontal pipe are compared with the Lee's correlation [7]. It shows that Lee's correlation slightly overestimates the present data for low j_g while underestimates for high j_g . It may be noted here that other correlations were examined but significantly poor agreement between the present data and predicted values was observed.

IV. Summary and Conclusions

Interfacial flow behavior for the countercurrent stratified two-phase flow of air-water has been experimentally investigated and f_i has been obtained from the force balance equations using measurements of pressure drop and water level. The main findings of the present work may be summarized as follows : (1) the presence of the hydraulic jump may significantly affect both the flow pattern and the value of f_i , (2) the important flow parameters that influence the evaluation of f_i are the relative velocity and the liquid level, (3) the measured values of f_i for nearly horizontal and two inclined pipe tests are the same order of magnitude but the dependency of f_i on the air and water velocities are slightly different, and (4) for nearly horizontal and two inclined pipe tests, distinct flow patterns are obtained when the air flow rate is increased while the water flow rate is fixed at constant value.

V. References

1. N. P. Cheremisinoff and E. J. Davis, "Stratified Turbulent-Turbulent Gas-Liquid Flow," *AICHE Journal*, Vol. 25, No. 1, pp. 48-56, 1979.
2. S. C. Lee and S. G. Bankoff, "Stability of Steam-Water Countercurrent Flow in an Inclined Channel: Flooding," *J. of Heat Transfer*, Vol. 105, pp. 713-718, 1983.
3. J. E. Kowalski, "Wall and Interfacial Shear Stress in Stratified Flow in a Horizontal Pipe," *AICHE Journal*, Vol. 33, No. 2, pp. 274-281, 1987.
4. H. J. Kim, S. C. Lee and S. G. Bankoff, "Heat Transfer and Interfacial Drag in Countercurrent Steam-Water Stratified Flow," *Int. J. Multiphase Flow*, Vol. 11, No. 5, pp. 593-606, 1985.
5. Andritsos and T. J. Hanratty, "Influence of Interfacial Waves in Stratified Gas-Liquid Flows," *AICHE Journal*, Vol. 33, No. 3, pp. 44-54, 1987.
6. Andreussi and L. N. Persen, "Stratified Gas-Liquid Flow in Downwardly Inclined Pipes," *Int. J. Multiphase Flow*, Vol. 13, No. 4, pp. 565-575, 1987.
7. S. C. Lee, "Interfacial Friction Factor in Countercurrent Stratified Two-Phase Flow," *Chem. Eng. Comm.*, Vol. 118, pp. 3-16, 1992.
8. M. H. Chun and H. Y. Nam, "An Experimental Investigation of the Adiabatic Interfacial Friction Factor in Horizontal Air-Water Countercurrent Stratified Flow," *Symposium on Transient Thermal Hydraulics, Heat Transfer and Coupled Vessel and Piping System Responses (1994 ASME Pressure Vessel and Piping Conference)*, Minneapolis Minnesota, June 19-23, 1994.

Table 1. Empirical Correlations for Interfacial Friction Factor

Author	Geometry	Correlation
Chermisinoff and Davis [1]	Cocurrent duct flow	$f_i = 0.0142$ $f_i = 0.008 + 2 \times 10^{-5} Re_f^2$ (for roll wave) $Re_f^* = \frac{f_i \pi D^2}{V_f 4 S_i}$
Lee and Bankoff [2]	Counter-current duct flow	$f_i = 0.012 + 5.179 \times 10^{-4} \frac{Re_g - Re_g^*}{1000}$, $Re_g < Re_g^*$ $f_i = 0.012 + 2.694 \times 10^{-4} \left(\frac{Re_f}{1000} \right)^{1.58} \frac{Re_g - Re_g^*}{1000}$, $Re_g > Re_g^*$ $Re_g^* = 1.837 \times 10^5 Re_f^{-0.184}$
Kowalski [3]	Cocurrent pipe flow	$f_i = 0.96(Re_g^*)^{-0.52}$ (for smooth surface) $f_i = 7.5 \times 10^{-5} (1 - \alpha)^{-0.23} Re_g^{-0.3} Re_f^{0.85}$ (for wavy surface) $Re_g^* = \frac{f_g D}{V_g}$, $Re_g = \frac{V_g D}{\nu}$, $Re_f = \frac{V_f D}{\nu}$
Kim et al. [4]	Counter-current duct flow	$f_i = 0.56 \times 10^{-5} Re_f + 0.084$
Andritsos and Hanratty [5]	Cocurrent pipe flow	$f_i/f_g = 1$ (for $j_k \leq j_{k,1}$) $f_i/f_g = 1 + 15 \left(\frac{h_f}{D} \right)^{1/2} \left(\frac{j_k}{j_{k,1}} - 1 \right)$ (for $j_k > j_{k,1}$) $j_{k,1} = 5 \left(\frac{\rho_{av}}{\rho_g} \right)^{1/2}$, $f_k = 0.046 Re_g^{-0.2}$
Andreussi and Persen [6]	Cocurrent pipe flow	$f_i/f_g = 1$ (for $F \leq 0.36$) $f_i/f_g = 1 + 29.7(F - 0.36)^{0.67} \left(\frac{h_f}{D} \right)^{0.2}$ (for $F > 0.36$) $F = V_f \left(\frac{\rho_x}{\Delta \rho} \frac{dA_f/dh_f}{A_p} \frac{1}{g \cos \theta} \right)^{1/2}$
Lee [7]	Counter-current duct flow	$f_i = 4.13 \times 10^{-11} Re_g^{0.96} Re_f^{0.76} \left(\frac{h_f}{D} \right)^{1.86}$ for three-dimensional wave regime
Chun and Nam [8]	Counter-current duct and pipe flow	$f_i = 0.01(3X)^{0.8+X}$ $X = 0.02 \left(\frac{V_g}{\sqrt{gD}} \right)^2 Re_f^{1/3} \left(\frac{D_{b,i}}{D + D_{b,i}} \right)^2$

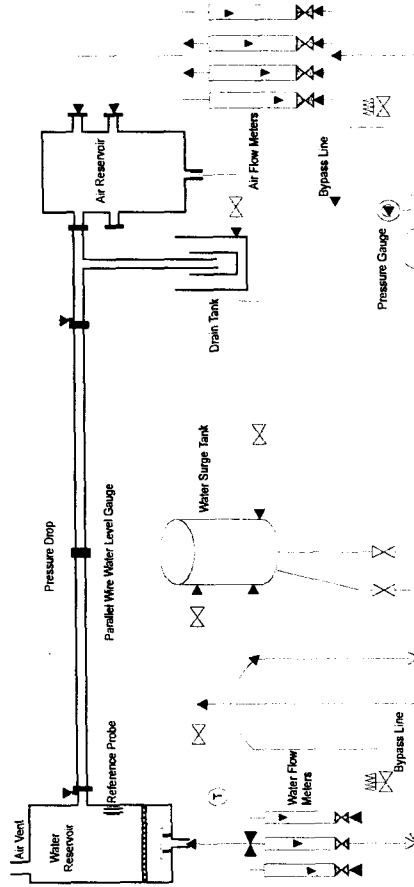


Figure 1. Schematic Diagram of Experimental Facility (Air/Water Loop).

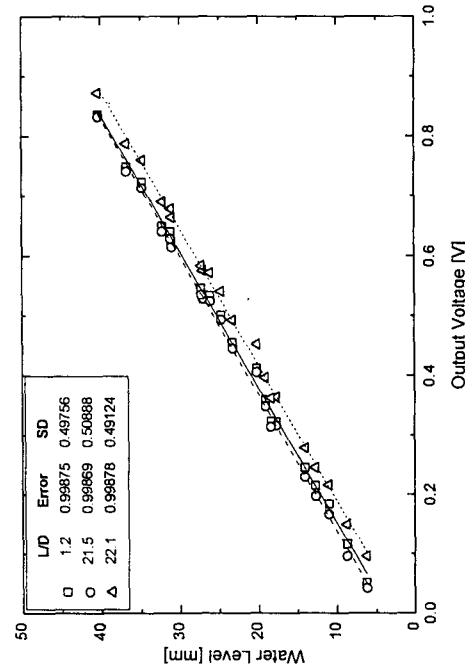


Figure 2. Calibration Curves for the Water Level Gauges.

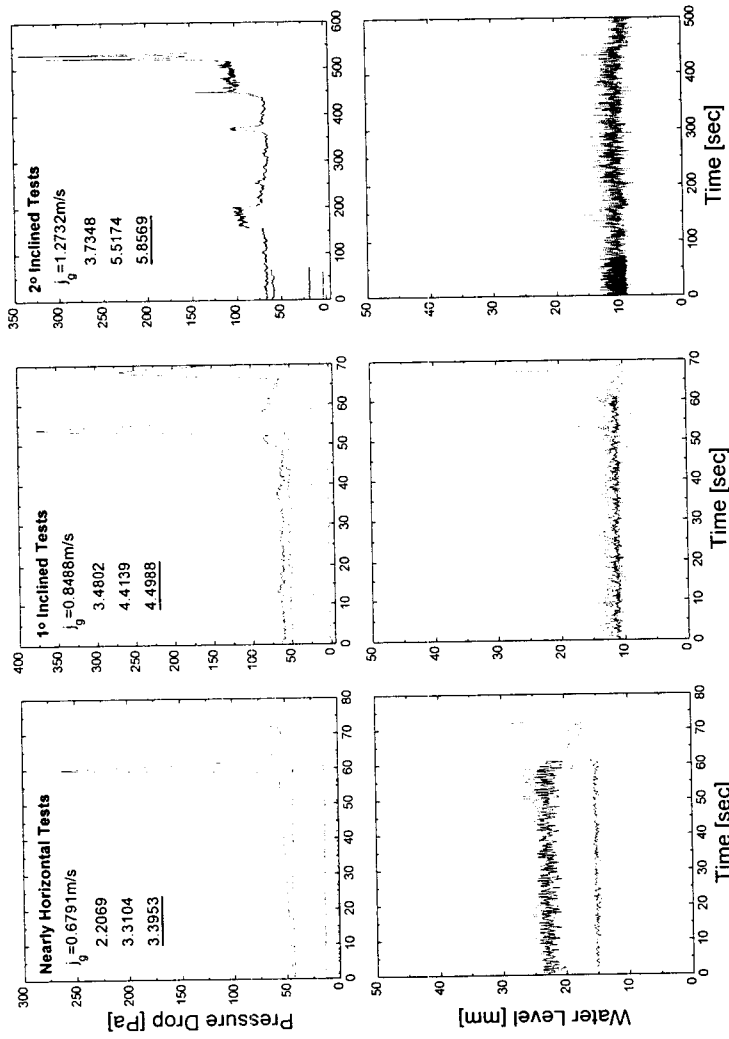


Figure 3. Behaviors of Pressure drop and Water Level for $j_g=0.0679\text{m/s}$.

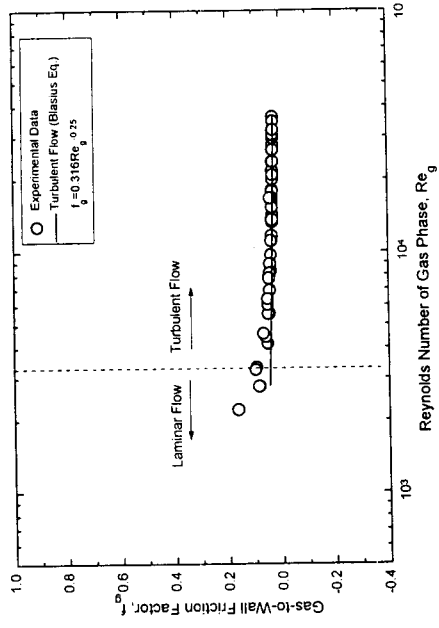
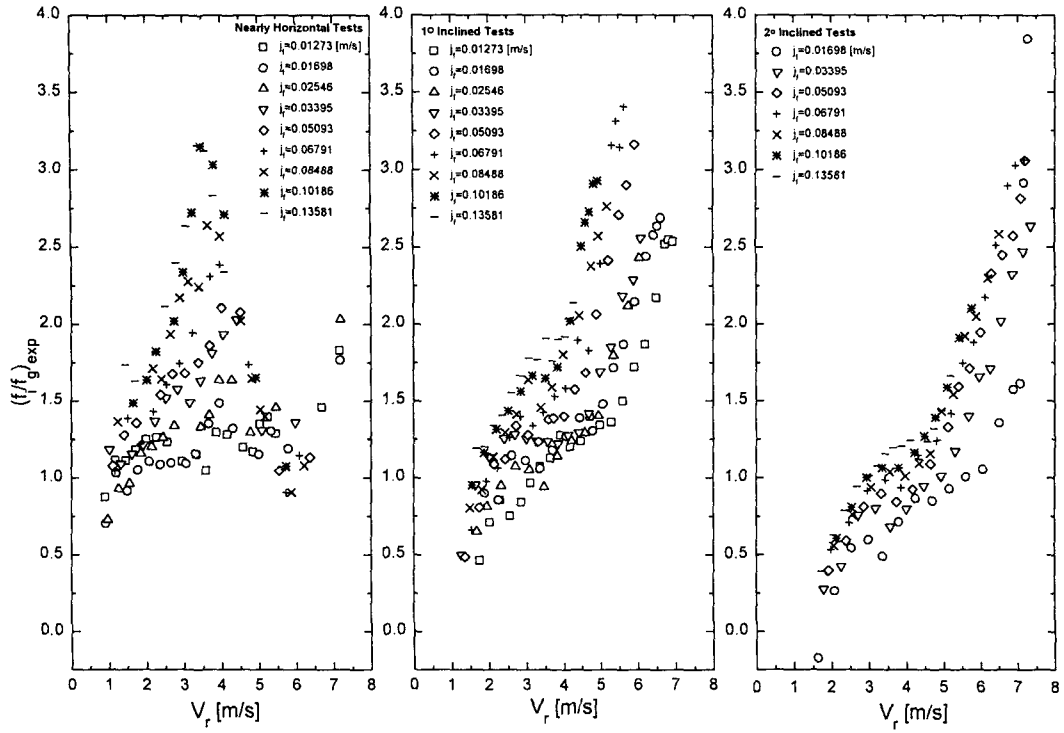


Figure 4. Comparison of Experimental Data of Gas-to-Wall Friction Factor with Blasius Equation.



(a) Nearly Horizontal Tests (b) 1° Inclined Tests (c) 2° Inclined Tests

Figure 5. Behavior of Interfacial Friction Factor as a Function of V_r .

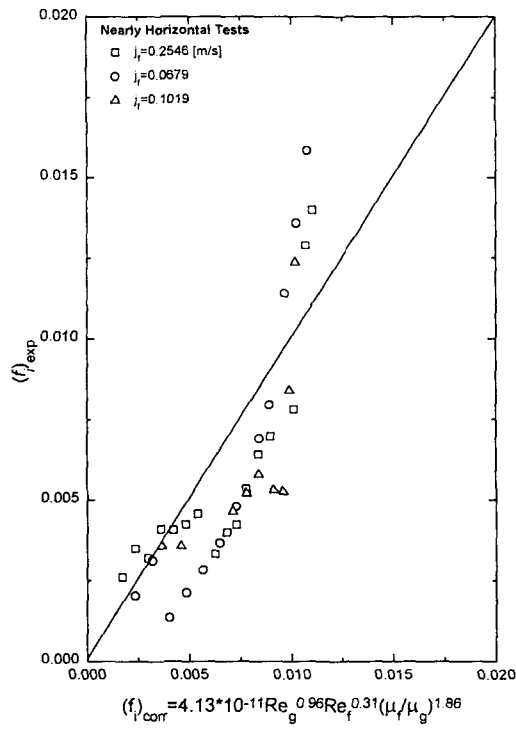


Figure 6. Comparison of Experimental Data with Lee's Correlation.